

Soil Moisture Retrieval using Sliced Regression Inversion Technique

Siddhant Gautam

Advisor: Prof. Uday K Khankhoje

Electrical Engineering,
Indian Institute of Technology Madras

December 18, 2020

Table of Contents

1 Introduction

2 Forward Model

3 Inverse Model

4 Results

- Synthetic Data
- Experimental Data

5 Conclusion

Soil Moisture - Why does it matter?

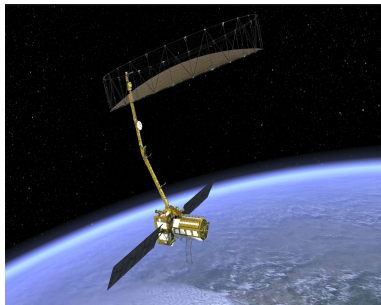


Figure: Applications of soil moisture measurements¹

¹Entekhabi, Dara, et al. "The soil moisture active passive (SMAP) mission." Proceedings of the IEEE 98.5 (2010): 704-716

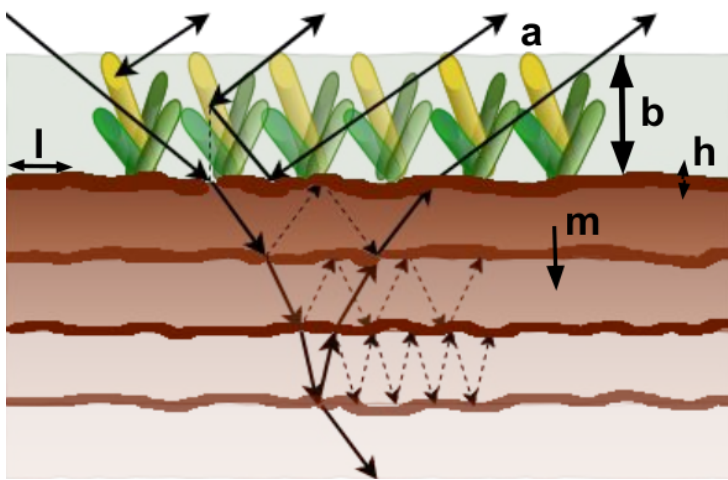
NASA-ISRO Synthetic Aperture Radar (NISAR) Mission²

- Joint Mission by ISRO-NASA (2021)
- Operated bands: L and S
- All-Weather Day and Night Imaging
- Mission Objectives:
 - ① Agricultural Monitoring
 - ② Glacier and coastal studies
 - ③ Disaster monitoring and assessment

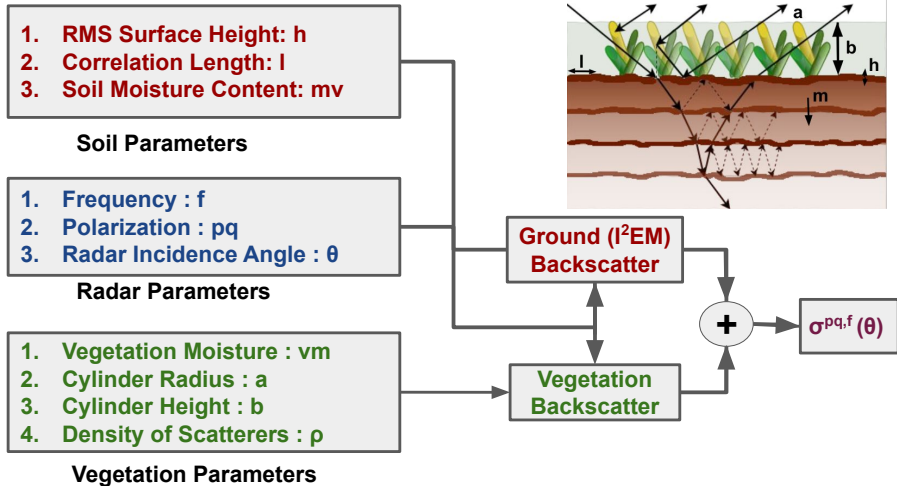


²Rosen, Paul A., et al. "Global persistent SAR sampling with the NASA-ISRO SAR (NISAR) mission." 2017 IEEE Radar Conference (RadarConf). IEEE, 2017

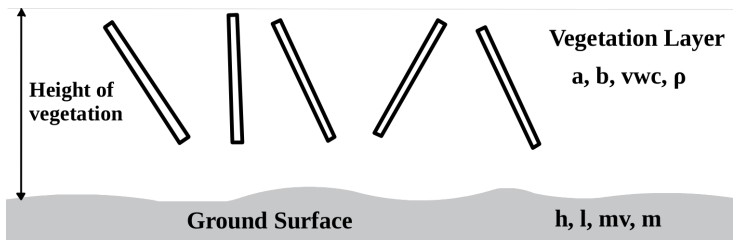
Forward Model - Schematic



Forward Model - Block Diagram

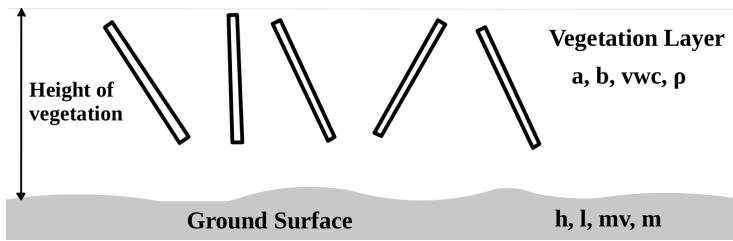


Modeling Vegetation Backscatter³



³van Zyl, Jakob J. Synthetic aperture radar polarimetry. Vol. 2. John Wiley & Sons, 2011.

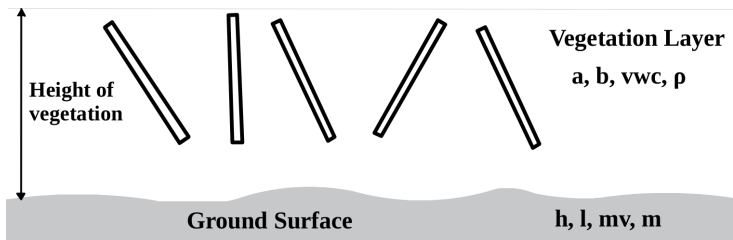
Modeling Vegetation Backscatter³



- A single layer vegetation model

³van Zyl, Jakob J. Synthetic aperture radar polarimetry. Vol. 2. John Wiley & Sons, 2011.

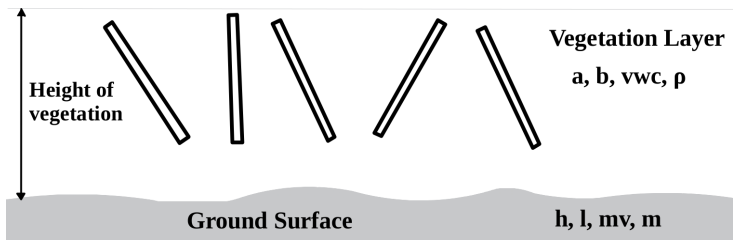
Modeling Vegetation Backscatter³



- A single layer vegetation model
- Describes scattering from grasslands, pasture lands, etc.

³van Zyl, Jakob J. Synthetic aperture radar polarimetry. Vol. 2. John Wiley & Sons, 2011.

Modeling Vegetation Backscatter³

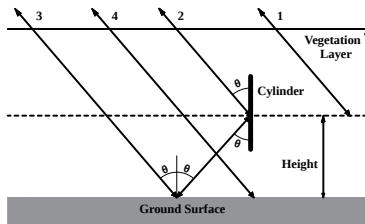


- A single layer vegetation model
- Describes scattering from grasslands, pasture lands, etc.
- Spatial distribution of cylinders governed by a cosine-squared PDF

³van Zyl, Jakob J. Synthetic aperture radar polarimetry. Vol. 2. John Wiley & Sons, 2011.

Single Layer Vegetation Model ⁴

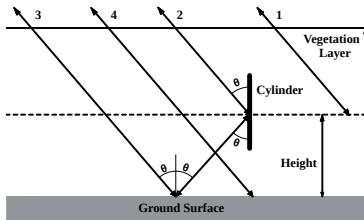
- ① Scattering from the Vegetation Layer **Path-1**
- ② Double Reflection Scattering Paths-**2,3**
- ③ Backscatter from the Ground Surface **Path-4**



⁴Freeman, Anthony, and Stephen L. Durden. "A three-component scattering model for polarimetric SAR data." IEEE TGRS (1998)

Single Layer Vegetation Model ⁴

- ① Scattering from the Vegetation Layer **Path-1**
- ② Double Reflection Scattering **Paths-2,3**
- ③ Backscatter from the Ground Surface **Path-4**



Backscatter Contributions from soil and vegetation

$$\sigma_{total} = \sigma_{veg}(vwc, a, b, \rho_s) + \tau^2 \sigma_{IEM}(h, l, \epsilon) + \sigma_{db}(vwc, a, b, \rho_s, h, l, \epsilon)$$

⁴Freeman, Anthony, and Stephen L. Durden. "A three-component scattering model for polarimetric SAR data." IEEE TGRS (1998)

Bistatic Scattering Matrix of a Cylinder⁵

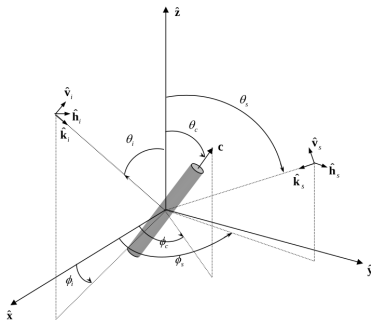


Figure: Global backscattering alignment coordinate system

Scattering Matrix

$$\mathbf{E}^{sc} = [\mathbf{S}] \mathbf{E}^{inc} \frac{e^{ikr}}{r}$$

where

$$\mathbf{S} = \begin{bmatrix} S_{HH} & S_{HV} \\ S_{VH} & S_{VV} \end{bmatrix}$$

⁵van Zyl, Jakob J. Synthetic aperture radar polarimetry. Vol. 2. John Wiley & Sons, 2011.

Vegetation Backscatter⁶

1. Scattering Coefficient of a Single Cylinder

$$S_{HH} = -\frac{il \sin \theta_s}{\pi \sin \theta_i} \frac{\sin V}{V} \sum_{m=-\infty}^{\infty} (-1)^m C_m^{TM} e^{im(\phi_s - \phi_i)}$$

⁶Arii, Motofumi. Retrieval of soil moisture under vegetation using polarimetric radar.
Diss. California Institute of Technology, 2009.

Vegetation Backscatter⁶

1. Scattering Coefficient of a Single Cylinder

$$S_{HH} = -\frac{il \sin \theta_s}{\pi \sin \theta_i} \frac{\sin V}{V} \sum_{m=-\infty}^{\infty} (-1)^m C_m^{TM} e^{im(\phi_s - \phi_i)}$$

2. Averaging over all possible orientations: $p(\theta_c, \phi_c) = 1/2\pi \cos^2 \theta_c$

$$\langle S_{HH} S_{HH}^* \rangle = \int_0^{2\pi} \int_0^\pi S_{HH} S_{HH}^* p(\theta_c, \phi_c) \sin \theta_c d\theta_c d\phi_c$$

⁶Arii, Motofumi. Retrieval of soil moisture under vegetation using polarimetric radar.
Diss. California Institute of Technology, 2009.

Vegetation Backscatter⁶

1. Scattering Coefficient of a Single Cylinder

$$S_{HH} = -\frac{il \sin \theta_s}{\pi \sin \theta_i} \frac{\sin V}{V} \sum_{m=-\infty}^{\infty} (-1)^m C_m^{TM} e^{im(\phi_s - \phi_i)}$$

2. Averaging over all possible orientations: $p(\theta_c, \phi_c) = 1/2\pi \cos^2 \theta_c$

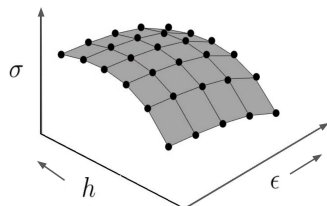
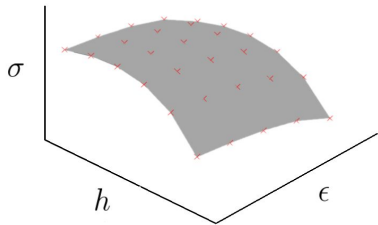
$$\langle S_{HH} S_{HH}^* \rangle = \int_0^{2\pi} \int_0^\pi S_{HH} S_{HH}^* p(\theta_c, \phi_c) \sin \theta_c d\theta_c d\phi_c$$

3. Calculating the Backscattering Coefficient

$$\sigma_{HH} = 4\pi \frac{b \rho_s \cos \theta_i}{4\tau_{thm}} \langle S_{HH} S_{HH}^* \rangle$$

⁶Arii, Motofumi. Retrieval of soil moisture under vegetation using polarimetric radar.
Diss. California Institute of Technology, 2009.

Sliced Regression Inversion Algorithm



SRI - Data Cube Generation

Data Cube Generation

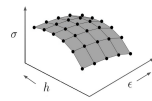
$$\sigma^{pq,f} = F(h_i, l_i, m_{v_i}, v_{m_i}, pq, f) \forall i \in \{1, n\}$$

SRI - Data Cube Generation

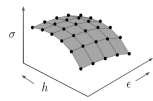
Data Cube Generation

$$\sigma^{pq,f} = F(h_i, l_i, m_{v_i}, v_{m_i}, pq, f) \forall i \in \{1, n\}$$

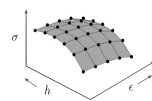
For polarization $pq = \{HH, VV, HV\}$ and frequency bands $f = L, S$:



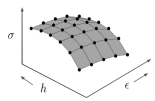
$\sigma^{HH,L}$



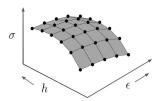
$\sigma^{HV,L}$



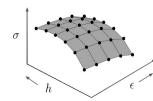
$\sigma^{VV,L}$



$\sigma^{HH,S}$



$\sigma^{HV,S}$



$\sigma^{VV,S}$

SRI - Inversion

$$\underbrace{\begin{bmatrix} \sigma_k^{HH,L} - \beta_{0,k}^{HH,L} \\ \vdots \\ \sigma_k^{HV,S} - \beta_{0,k}^{HV,S} \end{bmatrix}}_{\vec{z}} = \underbrace{\begin{bmatrix} \beta_{1,k}^{HH,L} & \dots & \beta_{d,k}^{HH,L} \\ \vdots & \ddots & \vdots \\ \beta_{1,k}^{HV,S} & \dots & \beta_{d,k}^{HV,S} \end{bmatrix}}_{\boldsymbol{\beta}} \underbrace{\begin{bmatrix} x_1 \\ \vdots \\ x_d \end{bmatrix}}_{\vec{x}}$$

SRI - Inversion

$$\underbrace{\begin{bmatrix} \sigma_k^{HH,L} - \beta_{0,k}^{HH,L} \\ \vdots \\ \sigma_k^{HV,S} - \beta_{0,k}^{HV,S} \end{bmatrix}}_{\vec{z}} = \underbrace{\begin{bmatrix} \beta_{1,k}^{HH,L} & \dots & \beta_{d,k}^{HH,L} \\ \vdots & \ddots & \vdots \\ \beta_{1,k}^{HV,S} & \dots & \beta_{d,k}^{HV,S} \end{bmatrix}}_{\boldsymbol{\beta}} \underbrace{\begin{bmatrix} x_1 \\ \vdots \\ x_d \end{bmatrix}}_{\vec{x}}$$

- Define $y = \bar{\sigma}^{pq,f} - \beta_{0,k}^{pq,f}$, where $\bar{\sigma}^{pq,f}$ is the value measured by SAR

SRI - Inversion

$$\underbrace{\begin{bmatrix} \sigma_k^{HH,L} - \beta_{0,k}^{HH,L} \\ \vdots \\ \sigma_k^{HV,S} - \beta_{0,k}^{HV,S} \end{bmatrix}}_{\vec{z}} = \underbrace{\begin{bmatrix} \beta_{1,k}^{HH,L} & \dots & \beta_{d,k}^{HH,L} \\ \vdots & \ddots & \vdots \\ \beta_{1,k}^{HV,S} & \dots & \beta_{d,k}^{HV,S} \end{bmatrix}}_{\beta} \underbrace{\begin{bmatrix} x_1 \\ \vdots \\ x_d \end{bmatrix}}_{\vec{x}}$$

- Define $y = \bar{\sigma}^{pq,f} - \beta_{0,k}^{pq,f}$, where $\bar{\sigma}^{pq,f}$ is the value measured by SAR
- Due to measurement noise and modelling errors, $\vec{y} \neq \beta \vec{x}$

SRI - Inversion

$$\underbrace{\begin{bmatrix} \sigma_k^{HH,L} - \beta_{0,k}^{HH,L} \\ \vdots \\ \sigma_k^{HV,S} - \beta_{0,k}^{HV,S} \end{bmatrix}}_{\vec{z}} = \underbrace{\begin{bmatrix} \beta_{1,k}^{HH,L} & \dots & \beta_{d,k}^{HH,L} \\ \vdots & \ddots & \vdots \\ \beta_{1,k}^{HV,S} & \dots & \beta_{d,k}^{HV,S} \end{bmatrix}}_{\beta} \underbrace{\begin{bmatrix} x_1 \\ \vdots \\ x_d \end{bmatrix}}_{\vec{x}}$$

- Define $y = \bar{\sigma}^{pq,f} - \beta_{0,k}^{pq,f}$, where $\bar{\sigma}^{pq,f}$ is the value measured by SAR
- Due to measurement noise and modelling errors, $\vec{y} \neq \beta \vec{x}$
- Find \vec{x} that explains the data with the least error

SRI - Inversion

$$\underbrace{\begin{bmatrix} \sigma_k^{HH,L} - \beta_{0,k}^{HH,L} \\ \vdots \\ \sigma_k^{HV,S} - \beta_{0,k}^{HV,S} \end{bmatrix}}_{\vec{z}} = \underbrace{\begin{bmatrix} \beta_{1,k}^{HH,L} & \dots & \beta_{d,k}^{HH,L} \\ \vdots & \ddots & \vdots \\ \beta_{1,k}^{HV,S} & \dots & \beta_{d,k}^{HV,S} \end{bmatrix}}_{\boldsymbol{\beta}} \underbrace{\begin{bmatrix} x_1 \\ \vdots \\ x_d \end{bmatrix}}_{\vec{x}}$$

- Define $y = \bar{\sigma}^{pq,f} - \beta_{0,k}^{pq,f}$, where $\bar{\sigma}^{pq,f}$ is the value measured by SAR
- Due to measurement noise and modelling errors, $\vec{y} \neq \boldsymbol{\beta}\vec{x}$
- Find \vec{x} that explains the data with the least error

Retrieving the soil moisture using the $\boldsymbol{\beta}$ for the k^{th} slice

$$\hat{\vec{x}} = \underset{\vec{x}}{\operatorname{argmin}} \|\vec{y} - \boldsymbol{\beta}\vec{x}\|^2 \text{ s.t. } \vec{x} \in \mathcal{B}_k$$

Retrieval Accuracy on Synthetic Dataset

Measurement	Vegetated Land		Bare Soil	
	RMSE	R2	RMSE	R2
[HH+HV]-L	0.11	0.44	0.14	0.14
[VV+VH]-S	0.11	0.45	0.12	0.29
[HH+VV]-[L,S]	0.09	0.66	0.07	0.71
[HH+VV+HV]-[L,S]	0.06	0.79	0.05	0.81

Table: Comparison of single and dual band soil moisture retrieval accuracy.

$h = [0.5 : 0.7 : 4]$ cm, $l = [5, 25]$ cm, $mv = [0.05 : 0.05 : 0.5]$ cm^3/cm^3 ,,
 $vm = [0.05 : 0.1 : 0.5]$ cm^3/cm^3 , $l_{\text{veg}} = [50 : 100 : 250]$ cm, $r_{\text{veg}} = [2 : 3 : 8]$ mm.

- **Error Metric:** RMSE - Root Mean Squared Error (cm^3/cm^3), R2 - Correlation Coefficient

Retrieval Accuracy on Synthetic Dataset

Measurement	Vegetated Land		Bare Soil	
	RMSE	R2	RMSE	R2
[HH+HV]-L	0.11	0.44	0.14	0.14
[VV+VH]-S	0.11	0.45	0.12	0.29
[HH+VV]-[L,S]	0.09	0.66	0.07	0.71
[HH+VV+HV]-[L,S]	0.06	0.79	0.05	0.81

Table: Comparison of single and dual band soil moisture retrieval accuracy.

$h = [0.5 : 0.7 : 4]$ cm, $l = [5, 25]$ cm, $mv = [0.05 : 0.05 : 0.5]$ cm^3/cm^3 ,
 $vm = [0.05 : 0.1 : 0.5]$ cm^3/cm^3 , $l_{\text{veg}} = [50 : 100 : 250]$ cm, $r_{\text{veg}} = [2 : 3 : 8]$ mm.

- **Error Metric:** RMSE - Root Mean Squared Error (cm^3/cm^3), R2 - Correlation Coefficient
- Dual band performs better than single band

Retrieval Accuracy on Synthetic Dataset

Measurement	Vegetated Land		Bare Soil	
	RMSE	R2	RMSE	R2
[HH+HV]-L	0.11	0.44	0.14	0.14
[VV+VH]-S	0.11	0.45	0.12	0.29
[HH+VV]-[L,S]	0.09	0.66	0.07	0.71
[HH+VV+HV]-[L,S]	0.06	0.79	0.05	0.81

Table: Comparison of single and dual band soil moisture retrieval accuracy.

$h = [0.5 : 0.7 : 4]$ cm, $l = [5, 25]$ cm, $mv = [0.05 : 0.05 : 0.5]$ cm^3/cm^3 ,
 $vm = [0.05 : 0.1 : 0.5]$ cm^3/cm^3 , $l_{\text{veg}} = [50 : 100 : 250]$ cm, $r_{\text{veg}} = [2 : 3 : 8]$ mm.

- **Error Metric:** RMSE - Root Mean Squared Error (cm^3/cm^3), R2 - Correlation Coefficient
- Dual band performs better than single band
- Adding cross polarized backscatter leads to better accuracy

NISAR Operating Bands (L and S) - Bare Soil

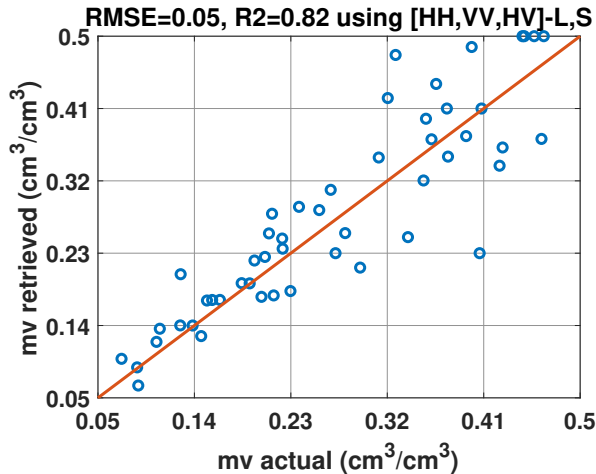


Figure: Scatter plot showing performance of SRI algorithm for soil moisture retrieval using dual (L+S) band (synthetic) data over bare soil

NISAR Operating Bands (L and S) - Vegetated Lands

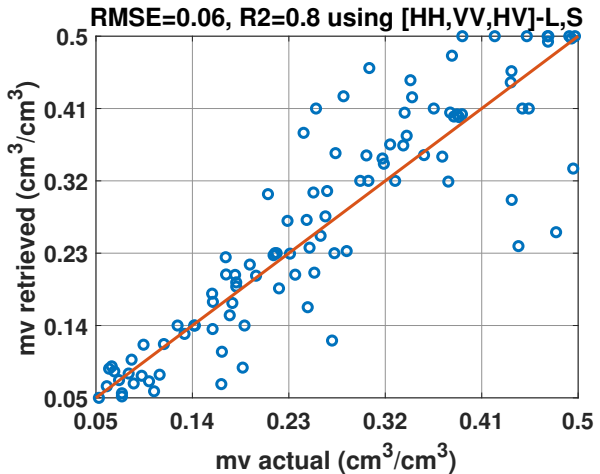


Figure: Scatter plot showing performance of SRI algorithm for soil moisture retrieval using dual (L+S) band (synthetic) data over vegetated soils

Ground Truth Data Collection

- **Collecting Agency:** Space Applications Centre (ISRO)
- **Collaborators:** Dharmendra Pandey & Shivani Tyagi - SAC/ISRO
- **Area:** Agriculture fields spread over Guntur, Andhra Pradesh
- **Satellites:** ALOS PALSAR (L-band), SENTINEL (C-band)



Accuracy on Real Dataset - Bare Soil and Maize Crop

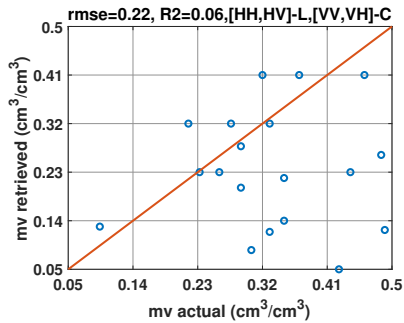
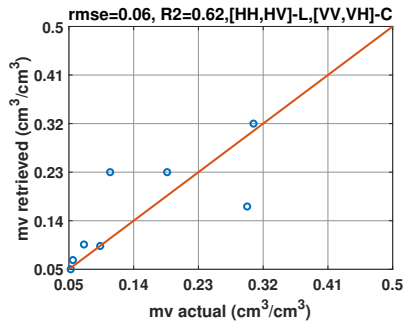


Figure: Retrieval accuracy of SRI for (1) bare soil and (2) maize crop using experimental data.

Accuracy on Real Dataset - Bare Soil and Maize Crop

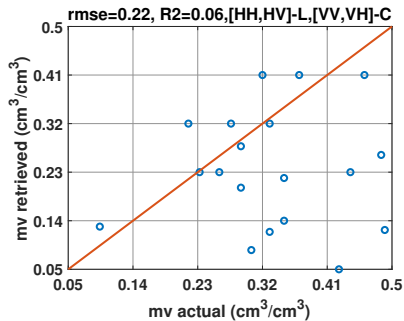
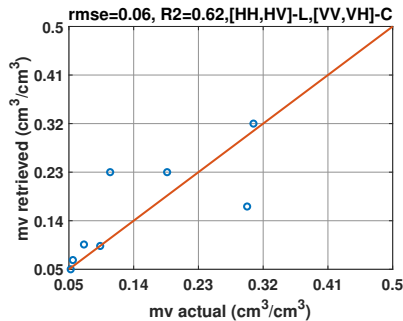


Figure: Retrieval accuracy of SRI for (1) bare soil and (2) maize crop using experimental data.

- For maize crop, the radius is fixed at 5mm and length is retrieved.

Accuracy on Real Dataset - Bare Soil and Maize Crop

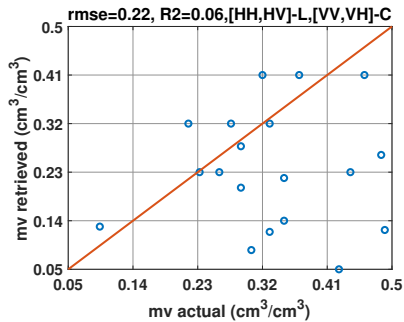
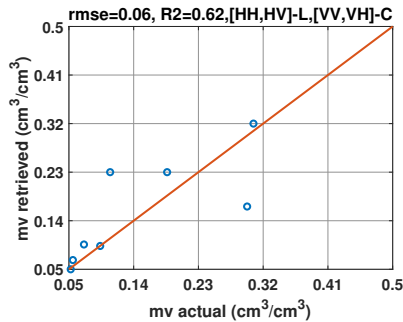


Figure: Retrieval accuracy of SRI for (1) bare soil and (2) maize crop using experimental data.

- For maize crop, the radius is fixed at 5mm and length is retrieved.
- There must be either a modelling error or an incorrect fixed parameter causing the mismatch.

Accuracy on Real Dataset - Chilli Crop

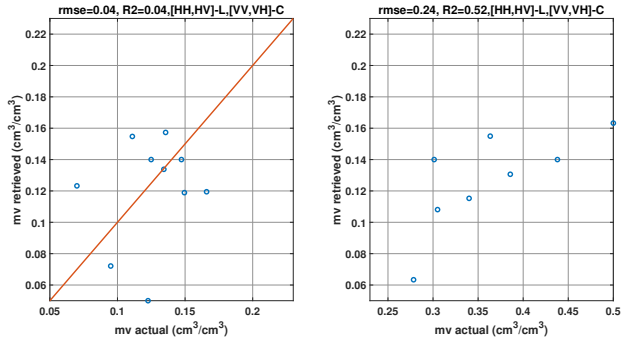


Figure: Retrieval accuracy of SRI approach for chilli crop using the experimental data. Cylinder radius and length are fixed at 2mm and 50 cm respectively.

Accuracy on Real Dataset - Chilli Crop

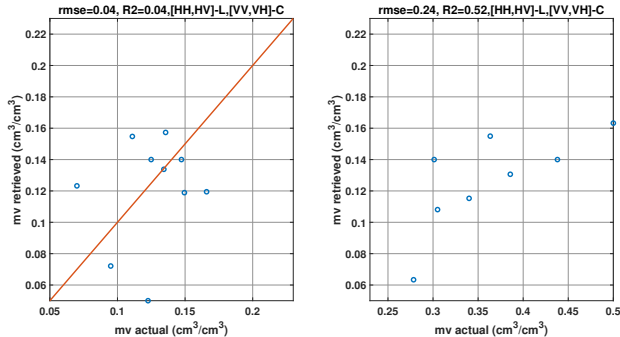


Figure: Retrieval accuracy of SRI approach for chilli crop using the experimental data. Cylinder radius and length are fixed at 2mm and 50 cm respectively.

- Low values of soil moisture ($mv < 0.25$) retrieved with good accuracy ($0.04 \text{ cm}^3/\text{cm}^3$)

Accuracy on Real Dataset - Chilli Crop

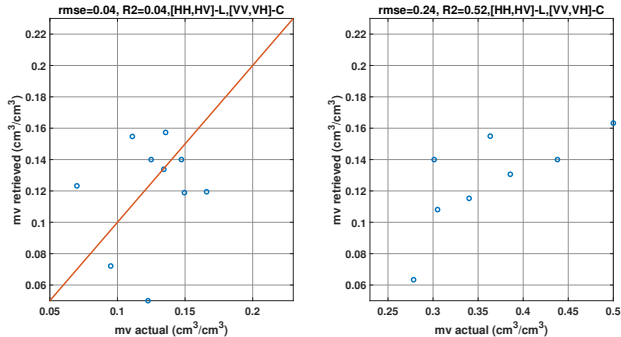


Figure: Retrieval accuracy of SRI approach for chilli crop using the experimental data. Cylinder radius and length are fixed at 2mm and 50 cm respectively.

- Low values of soil moisture ($mv < 0.25$) retrieved with good accuracy ($0.04 \text{ cm}^3/\text{cm}^3$)
- For wet soil with moisture content greater than $0.25 \text{ cm}^3/\text{cm}^3$, accuracy is poor.

Comparison with LUT approach [Seung-Bum Kim 2013]

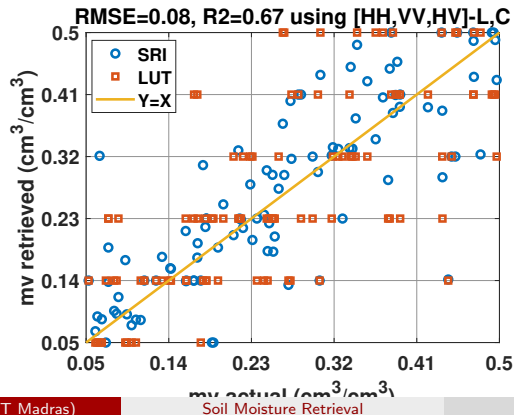
Algorithm	Maize	Chilli	Jowar	Bare Soil
SRI	0.2	0.18	0.26	0.06
LUT	0.43	0.27	0.47	0.17

Table: Retrieval Accuracy using the ALOS-PALSAR (L-band) and SENTINEL-1A (C-band) data.

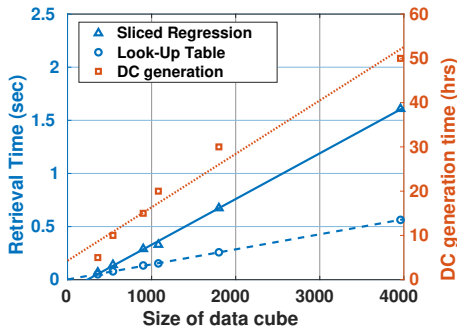
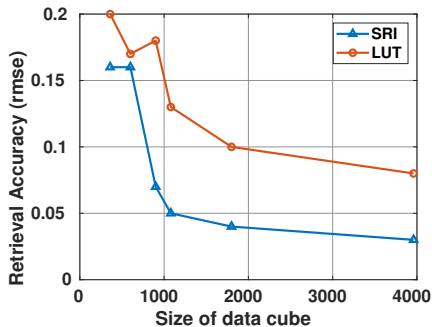
Comparison with LUT approach [Seung-Bum Kim 2013]

Algorithm	Maize	Chilli	Jowar	Bare Soil
SRI	0.2	0.18	0.26	0.06
LUT	0.43	0.27	0.47	0.17

Table: Retrieval Accuracy using the ALOS-PALSAR (L-band) and SENTINEL-1A (C-band) data.

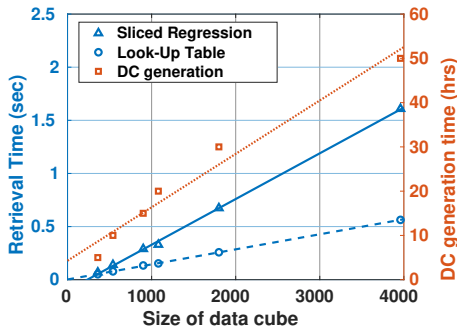
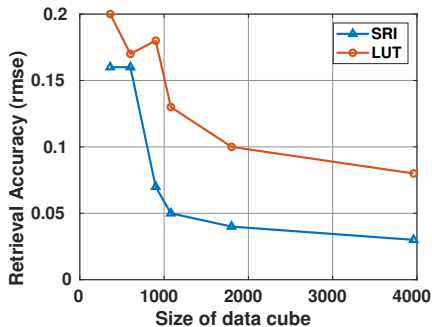


Accuracy and Time Consideration - SRI vs LUT⁷



⁷Kim, Seung-Bum, et al. "Models of L-band radar backscattering coefficients over global terrain for soil moisture retrieval." IEEE Transactions on Geoscience and Remote Sensing 52.2 (2013): 1381-1396.

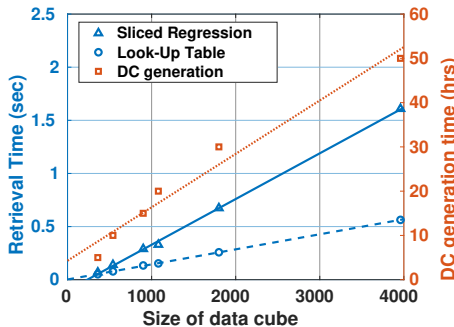
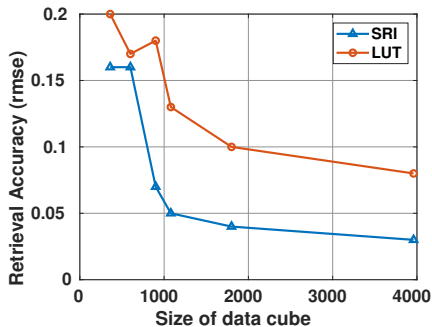
Accuracy and Time Consideration - SRI vs LUT⁷



- Linear dependence of retrieval time on datacube size

⁷Kim, Seung-Bum, et al. "Models of L-band radar backscattering coefficients over global terrain for soil moisture retrieval." IEEE Transactions on Geoscience and Remote Sensing 52.2 (2013): 1381-1396.

Accuracy and Time Consideration - SRI vs LUT⁷



- Linear dependence of retrieval time on datacube size
- For a given RMSE, DC generation time different-SRI:20 hrs,LUT:50 hrs

⁷Kim, Seung-Bum, et al. "Models of L-band radar backscattering coefficients over global terrain for soil moisture retrieval." IEEE Transactions on Geoscience and Remote Sensing 52.2 (2013): 1381-1396.

Conclusion

- Presented a new soil moisture inversion algorithm, termed Sliced Regression Inversion
 - Approximates the relationship between the backscatter and physical parameters by piece-wise linear models
 - Performs linear regression within each slice to obtain an estimate of the physical parameters
 - Picks physical parameters that minimize the residual error

Conclusion

- Presented a new soil moisture inversion algorithm, termed Sliced Regression Inversion
 - Approximates the relationship between the backscatter and physical parameters by piece-wise linear models
 - Performs linear regression within each slice to obtain an estimate of the physical parameters
 - Picks physical parameters that minimize the residual error
- Physics-based forward model with broader range of applicability than empirical models (limited guarantee and site specific validity)

Conclusion

- Presented a new soil moisture inversion algorithm, termed Sliced Regression Inversion
 - Approximates the relationship between the backscatter and physical parameters by piece-wise linear models
 - Performs linear regression within each slice to obtain an estimate of the physical parameters
 - Picks physical parameters that minimize the residual error
- Physics-based forward model with broader range of applicability than empirical models (limited guarantee and site specific validity)
- Proposed algorithm validated against experimental data with 6% and 13% accuracy for bare soils and vegetated lands

Conclusion

- Presented a new soil moisture inversion algorithm, termed Sliced Regression Inversion
 - Approximates the relationship between the backscatter and physical parameters by piece-wise linear models
 - Performs linear regression within each slice to obtain an estimate of the physical parameters
 - Picks physical parameters that minimize the residual error
- Physics-based forward model with broader range of applicability than empirical models (limited guarantee and site specific validity)
- Proposed algorithm validated against experimental data with 6% and 13% accuracy for bare soils and vegetated lands
- SRI more accurate and computationally efficient than the lookup table approach

Publications

Manuscripts under Preparation:

- ① **Siddhant Gautam, Dharmendra K Pandey, Uday K Khankhoje, "Soil Moisture Retrieval from Multi-Frequency Multi-Polarization SAR Data Using a Sliced Regression Inversion Technique"**

Peer Reviewed Conferences:

- ① **Gautam, S., S. V. Chidambaram, N. Gunturu, and U. K. Khankhoje, Retrieval of soil moisture using sliced regression inversion technique.** In 2019 Photonics and Electromagnetics Research Symposium-Spring (PIERS-Spring). IEEE, 2019